Tracking small unmanned aerial vehicles using weather radar

Krzysztof Orzeł[1], David Pepyne[1], Sean Turner[1], Jezabel Vilardell Sanchez[1], Apoorva Bajaj[1], Michael Zink[1], and Stephen Frasier[1]

[1]*University of Massachusetts, Amherst, MA 01003, USA*

(Dated: 22 June 2018)

Krzysztof Orzeł

1. Introduction

The Federal Aviation Administration (FAA) estimates that by 2021 as many as six million small Unmanned Aerial Vehicles (sUAVs) or micro-drones could be in U.S. skies. This trend has been driven by the ease of regulations, availability of low-cost micro-drones, capabilities such as aerial reconnaissance and maneuverability, innovative uses of these systems, such as inspections of pipelines and utility lines, law enforcement and package delivery. At the same time, however, micro-drones increasingly have been creating problems that jeopardize public safety, business continuity and privacy concerns. Drone safety incidents, including flying improperly, or getting too close to other aircraft, now average about 250 a month (Levin, 2017). A counter-drone industry has developed around drone surveillance, or the monitoring and tracking of non-cooperative sUAVs (Holland-Michel, 2018).

The Center for Collaborative Adaptive Sensing of the Atmosphere (CASA) at the University of Massachusetts, Amherst has pioneered the innovative use of X-band dual polarization weather radar to detect, classify and track sUAVs (Orzel et al., 2017). Since most sUAV parts are made of carbon fiber, plastic and styrofoam, this class of drones is characterized by a very small radar cross section (RCS) between -30dBsm and -10dBsm (Schroder et al., 2015)(Chenchen and Hao, 2016). SUAVs exhibit a characteristic micro-Doppler signature that can be used for detection and for discrimination from avian targets such as birds (Werth, 2016). Tracking drones or birds, either in software or visually on a display, also requires a very fast update rate on order of 5 seconds. This necessitates the use of next generation multi-function phased array radar (MPAR) (Stailey and Hondl, 2016) or low-power radar network (Adams, 2018).

The radar being used in this project is a Phase Spin Weather Radar (PSWR) (Orzel and Frasier, 2018), which is located on campus of the University of Massachusetts at Amherst. PSWR is a dual polarization, X-band, 1D phased array radar. Dual-polarization is a current standard in weather radar industry and can be used to improve target classification (Torvik et al., 2016). PSWR in its current configuration is able to perform simultaneously a full 360 degree mechanical scan in the azimuth and a 90 degree (ground to zenith) electronic scan in the elevation. Hence a complete coverage of airspace can be achieved and the site revisit time is significantly reduced. Due to the size of an antenna and the transmitter power weather radars are well equipped to detect small airborne targets. On the other hand range resolution on order of 50-150 meters impedes radar ability to operate in the multi-target scenario such as drone swarms.

The rest of this paper is organized as follows. Section 2 focuses on the detection and classification techniques used in this work. In section 3 the results from different drone flight tests will be presented and the performance of a tracking algorithm will be compared to the UAV GPS log. Section 4 presents conclusions and recommendations for future work.

2. Detection and classification

Mechanical vibrations or rotations of structures on a target introduce frequency modulation on the radar return known as the micro-Doppler phenomenon (Chen et al., 2006). It can be expected that the signature of a multi-rotor UAV is related to the signature of a helicopter. For a helicopter the spectral signature is composed of a strong but narrow main body (ie fuselage and hub) Doppler component, which corresponds to the velocity of the helicopter and a much wider, but weaker Doppler components contributed by the rotating blades. Chen (2011) provides formula for a maximum Doppler shift induced by a rotating blade:

$$\begin{aligned} V_{tip} &= 2\pi L\Omega \\ f_{D_{max}} &= (2V_{tip}/\lambda)cos\beta \end{aligned} \tag{2.1}$$

where the velocity of the blade tip V_{tip} is a product of blade length L and rotation rate Ω. The maximum Doppler shift $f_{D_{max}}$ is scaled by a radar wavelength λ and the elevation angle β. A popular commercial drone, that crashed on the grounds of the White House (Shear and Schmidt, 2015), has a blade radius of 12 cm and rotation rate between 100 (hover) and 150 (max speed) revolutions per second, which results in a maximum Doppler shift of 4.95 and 7.43 kHz respectively. Thus, the

Table 1: Pseudocode for I,Q signal processing.

1. Get I,Q samples for current dwell and apply pulse compression. For the experiments the PSWR was operated in an alternating dual-polarization mode, 128 pulses per dwell (64 at each polarization) were collected at a PRF of 3000 Hz (1500 Hz per polarization). Given the X-band transmit frequency, this gives a Doppler velocity range of $\pm 12 m/s$ per polarization.
2. Calculate the micro-Doppler spectrum for each polarization using the modified periodogram method with a Hann window.
3. Implement 1D CA-CFAR in range for each spectral coefficient. This gives a pattern of detections for each range gate that represents the locations of the peaks in the micro-Doppler spectrum.
4. Use the pattern of detections in each range gate to decide if a "drone signature" is present. One way to do this is simply to count the number of detections in a range gate and announce detection when the count exceeds a certain threshold. Due to folding we expect spectral components induced by rotating blades in each Doppler gate (subject to signal to noise ratio). This can effectively isolate drones from other targets like birds, clutter, planes, and cars which tend to give a pattern of detections with a very small count. We also note that this technique can to some degree detect slow moving drones in clutter when the blade signatures are visible to either side of the clutter spike.
5. Report target (range gate, azimuth, time and number of detections in a range gate) to a down stream tracker.

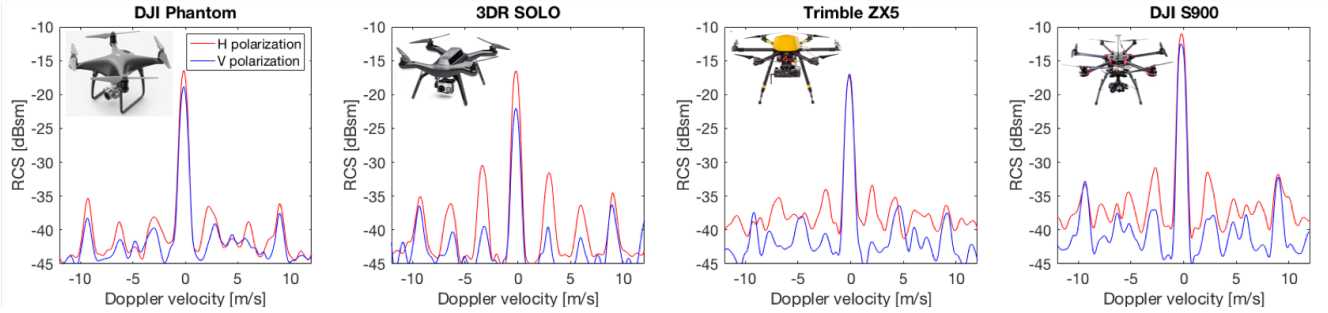

Figure 1: Micro-Doppler signatures of different UAV targets.

Nyquist sampling rate on order of 15 kHz is required. This is not feasible with the operational long-range weather radar and as a consequence folding in Doppler spectrum is expected.

In our study 4 different UAVs were examined: 2 quadcopters (DJI Phantom 4 and 3DR Solo) and 2 hexacopters (Trimble ZX5 and DJI S900). Each UAV micro-Doppler signature was aligned to the zero-Doppler velocity bin and then multiple measurements were accumulated in order to average out the RCS aspect angle dependence. The mean signatures are presented in Figure 1 and the key parameters are listed in Table 2. We note that horizontal polarization is preferable for drone detection. It provides higher measured main body RCS in 3 out of 4 cases. This was verified by Chenchen and Hao (2016) in their investigation of the dependence of RCS on polarization. They noted that the return strength from the battery pack has decreased, but the return strength from the drone motors have increased when horizontal- instead of vertical polarization was utilized. Ritchie et al. (2015) reported that significantly different RCS values (up to 30 dB in flashes at $f_c = 10 GHz$) of rotating DJI blades can be expected for horizontal and vertical polarizations. The micro-Doppler signature is more prevalent in H-channel, although for DJI Phantom the difference is subtle to notice. All UAV signatures are symmetrical, while bird signature tends to be asymmetric (de Wit et al., 2014). The biggest UAV (ie DJI S900) exhibits the highest RCS as expected. The main body RCS is between -10 and -20 dBsm, which is in a good agreement with previously reported values. The micro-Doppler components in the spectrum are between -45 and -30 dBsm. In general, the micro-Doppler signature can be effectively used for target classification, if sufficient system sensitivity can be guaranteed.

Several researchers (Molchanov et al., 2013)(de Wit et al., 2014) proposed short time Fourier transform (STFT) based methods for UAV feature extraction. Oh et al. (2018) provides a thorough comparison of the state-of-the-art UAV classification

Table 2: Radar cross section of different commercial small UAVs measured by PSWR in horizontal and vertical polarization. All values present the mean over several (50+) measurements at different target aspect angles. Peak sidelobe level (PSL) indicates the peak spectral return related to the spinning blades. RCS indicates the peak spectral return related to the main body.

Parameter	DJI Phantom 4	3DR Solo	Trimble ZX5	DJI S900
$RCS_H[dBsm]$	-16.4	-16.6	-17.3	-11.1
$RCS_V[dBsm]$	-18.9	-22.1	-17	-12.5
$RCS_H - RCS_V[dB]$	2.5	5.5	-0.3	1.4
$PSL_H[dBsm]$	-35.3	-30.5	-33.4	-30.8
$PSL_V[dBsm]$	-37.5	-36.3	-36.4	-32.2

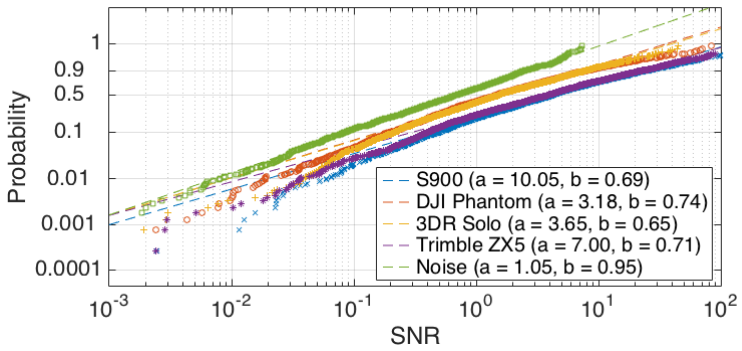

Figure 2: Weibull probability density function for different UAV targets and noise samples.

Table 3: PSWR tracking performance of DJI S900 target. The altitude is related to the UAV take off location, which was approximately 45 meters below radar site. The video of UAV tracking is available at: https://vimeo.com/275839325

Date	Mission	Altitude [m]	Range [m]	$\mu_r[m]$	σ_r	$\mu_{az}[^\circ]$	σ_{az}
2017/12/15	*Flight*#4	80-110	1050-1200	2.46	3.43	−0.13	0.72
	Flight#5	110	950-1250	0.7	5.17	−0.35	0.67
2018/04/24	*Flight*#1	100	950-1200	−0.14	2.91	−0.28	0.94
	Flight#2	100	900-1200	0	4.64	−0.17	0.87
	Flight#3	120	950-1200	0.06	4.57	−0.32	0.96
2018/06/12	*Flight*#1	90	1000-1500	−0.13	7.04	−0.08	1.67
	Flight#2	50-100	950-1200	−0.75	4.39	0.64	1.3

methods. These techniques are effective if a long duration target observation or/and high pulse repetition frequency (PRF) can be implemented. The future multi-function radar systems will be able to implement these techniques to some extent, but PSWR in its current configuration is not capable to provide the required quality of data due to slow pedestal movement and limited PRF. For this paper, the detection scheme used involved a simple cell averaging constant false alarm rate (CA-CFAR) algorithm performed in range-Doppler domain followed by an extraction of targets which present a general micro-Doppler signature. The procedure is presented in Table 1.

The statistics of data used to generate mean micro-Doppler signatures are investigated using the Weibull distribution. The Doppler component of the main body is excluded from these computations. The probability density function (pdf) of a Weibull random variable is given by:

$$f(x|a,b) = \frac{b}{a}\left(\frac{x}{a}\right)^{b-1} e^{-(x/a)^b} \quad x \geq 0 \tag{2.2}$$

where a is scale parameter and b is a shape parameter. The larger the scale parameter, the more spread out the distribution. If the data in x has a Weibull distribution, then the data is located along the reference line defined by a shape parameter in pdf. Distributions other than Weibull will introduce curvature in the plot. The probability density functions for 4 UAVs are presented in Figure 2. Additionally, for a reference we add PSWR noise data (green line), which should be exponentially distributed (b=1). The shape parameter of b=0.95 and scale parameter of a=1.05 confirm that noise samples have a Weibull distribution. On the other hand UAV data fit exhibits slight curvature for SNR > 10. The shape parameter is in range 0.65 and 0.74. Furthermore, we observe a noticeable difference in scale parameters, which allows to visually separate quadcopters form hexacopters.

3. Tracking

The output of the detection algorithm in the previous section becomes the input to a tracker. A challenge with tracking drones is they can move fast, slow, hover, turn suddenly, move up and down rapidly, etc. It is thus hard to come up with motion models for drones. One way to deal with drones is via fast update rate, since all motion looks locally linear when viewed at a high enough sample rate. Since our system didn't have a particularly fast update rate (approximately 15 seconds per PPI sweep), the tracking algorithm is based on Global Nearest Neighbor (GNN) approach, which attempts to find and to propagate the single most likely hypothesis at each scan (Konstantinova et al., 2003). The first detection is placed in its own track e.g. Track 1. Then the next detection is compared to Track 1. If that new detection being compared is too far away based on a distance threshold it will be placed into a new track. Each detection is compared to the last point of all the created tracks and then assigned to the track which it is closest to. This method worked reliably due to low number of targets and fairly low speed of UAV (3-6 m/s).

During the project several field campaigns were conducted. PSWR based tracking performance is presented in Table 3. DJI S900 target was flown between between 1000 and 1500 meters from the radar at various altitudes. The height of the drone

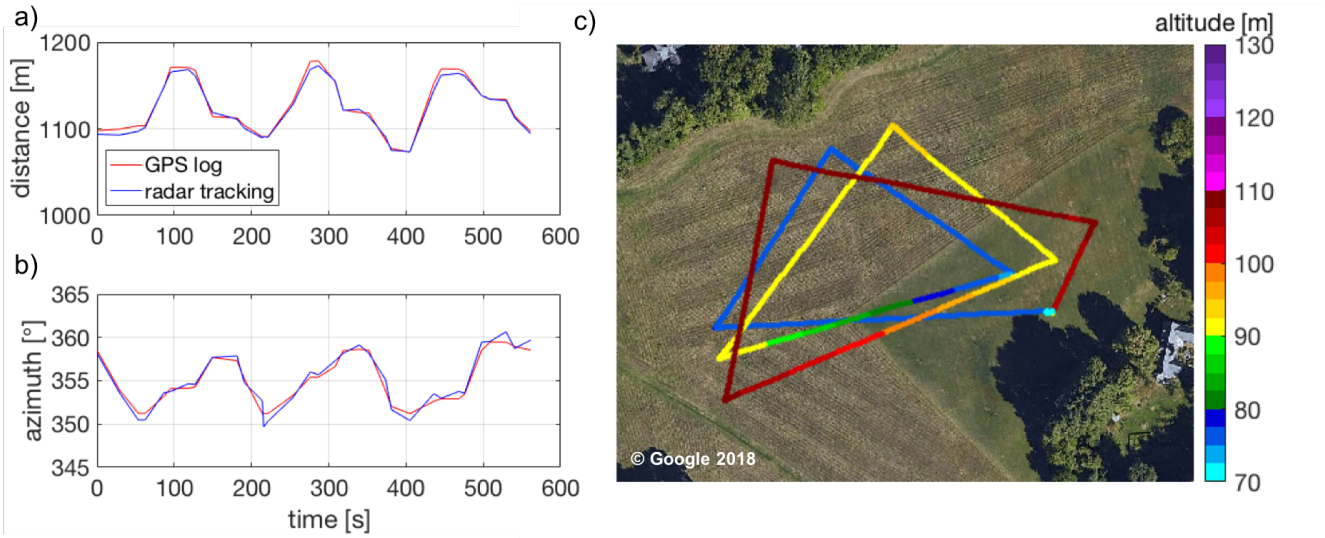

Figure 3: Flight #4 conducted on 2017/12/15: a) distance measured by radar- b) azimuth measured by radar compared with UAV GPS log. Panel c) presents the overlay of GPS track on a satellite picture. The drone ascended from 80 to 110 meters above ground level during the mission.

launch field was approximately 45 meters below the height of the radar site. In comparison to the GPS position data recorded on board of the drone, the mean error in range μ_r is in most cases below 1 m and the standard deviation of range estimation σ_r is smaller than 7m. The mean error in azimuth μ_{az} is smaller than 0.7° and the standard deviation of azimuth estimation σ_r is less smaller 1.7°.

This good tracking performance is illustrated in Figure 3 . For this mission the drone was hovering for 30 seconds in each corner and then progressing to the next one with a speed of 5m/s. The hover state is indicated by flat sections in Figure 3a and b. Hovering drone presents a clutter like target centered at zero-Doppler bin, but the micro-Doppler signature still allows for target detection. Our major issue was an aging mechanical pedestal, which prevented efficient tracking of high speed UAVs. Therefore, a phased array system with an electronic beam steering in azimuth or both azimuth and elevation would have been a better choice. It would then be possible to make the beam revisit the target location as frequently as needed.

4. Conclusions

This paper described the development of algorithms for the automated detection, classification, and tracking of sUAV with a low power, dual polarized, pulse doppler weather radar. Detection and classification was based on the identification of the micro-Doppler signature characteristic of copter-type targets. The algorithm was shown to work well for a variety of 4 rotor and 6 rotor drones. We observed that on average horizontal polarization promises higher chance of UAV detection. The tracker was based on a GNN approach. It worked well despite the low revisit time on order of 15 seconds, but needs to be modified to enable high speed UAV tracking. Future work is needed to explore detection and tracking of drone swarms (multiple close together drones that may or may not split and join during flight). Furthermore, detection in high urban clutter should be investigated. Use of electronic scanning is also preferable for an efficient clutter filtering as well as UAV and birds discrimination. We have demonstrated that functionality can be added to weather radar during "clear air" days when no severe weather is expected, and the radar can be used for micro-drone surveillance. This multi-function capability (weather and drone surveillance) could make such systems cost-effective for use in urban environments where these airborne hazards endanger lives and property.

Acknowledgment

The authors are grateful to the UAV pilots Silas Hughes, Daniel Myers and Ryan Wicks for the safe and smooth operations. We thank Eric Lyons for his help related to radar network communication. This work was supported by NSF Partnerships for Innovation - Accelerating Innovation Research Technology Transfer Award Number 1700967. Any opinions, findings, conclusions, or recommendations expressed in this material are those of the authors and do not necessarily reflect those of the NSF.

References

E. Adams, “Raytheon’s New Radar Could Bring Flying Cars and Drones to Our Cities,” 2018. [Online]. Available: https://www.wired.com/story/raytheon-radar-drones/

V. C. Chen, F. Li, S. S. Ho, and H. Wechsler, "Micro-Doppler effect in radar: phenomenon, model, and simulation study," *IEEE Transactions on Aerospace and Electronic Systems*, vol. 42, no. 1, pp. 2–21, Jan. 2006.

V. C. Chen, *The Micro-doppler Effect in Radar*. Artech House, 2011, google-Books-ID: eJ7eMHpxt30C.

J. L. Chenchen and L. Hao, "An Investigation on the Radar Signatures of Small Consumer Drones," *IEEE Antennas and Wireless Propagation Letters*, 2016.

J. de Wit, R. Harmanny, and P. Molchanov, "Radar micro-Doppler feature extraction using the Singular Value Decomposition," in *Radar Conference (Radar), 2014 International*, Oct. 2014, pp. 1–6.

A. Holland-Michel, *Counter Drone Systems*, Feb. 2018. [Online]. Available: http://dronecenter.bard.edu/files/2018/02/CSD-Counter-Drone-Systems-Report.pdf

P. Konstantinova, A. Udvarev, and T. Semerdjiev, "A Study of a Target Tracking Algorithm Using Global Nearest Neighbor Approach," in *Proceedings of the 4th International Conference Conference on Computer Systems and Technologies: E-Learning*, ser. CompSysTech '03. New York, NY, USA: ACM, 2003, pp. 290–295. [Online]. Available: http://doi.acm.org/10.1145/973620.973668

A. Levin, "Surge in Drone Safety Reports Prompts Emergency Action at FAA," *Bloomberg.com*, Oct. 2017. [Online]. Available: https://www.bloomberg.com/news/articles/2017-10-13/surge-in-drone-safety-reports-prompts-emergency-action-at-faa

P. Molchanov, K. Egiazarian, J. Astola, R. Harmanny, and J. de Wit, "Classification of small UAVs and birds by micro-Doppler signatures," in *Radar Conference (EuRAD), 2013 European*, Oct. 2013, pp. 172–175.

B. S. Oh, X. Guo, F. Wan, K. A. Toh, and Z. Lin, "Micro-Doppler Mini-UAV Classification Using Empirical-Mode Decomposition Features," *IEEE Geoscience and Remote Sensing Letters*, vol. 15, no. 2, pp. 227–231, Feb. 2018.

K. A. Orzel and S. J. Frasier, "Weather Observation by an Electronically Scanned Dual-Polarization Phase-Tilt Radar," *IEEE Transactions on Geoscience and Remote Sensing*, vol. 56, no. 5, pp. 2722–2734, May 2018. [Online]. Available: https://ieeexplore.ieee.org/document/8244253/

K. A. Orzel, S. Govindasamy, A. Bennett, D. Pepyne, and S. Frasier, "Detection and identification of the Remotely Piloted Aircraft System using a weather radar," *AMS 38th Conference on Radar Meteorology*, Aug. 2017. [Online]. Available: https://ams.confex.com/ams/38RADAR/meetingapp.cgi/Paper/321077

M. Ritchie, F. Fioranelli, and H. Griffiths, "Micro-Drone RCS Analysis," 2015.

A. Schroder, M. Renker, U. Aulenbacher, A. Murk, U. Boniger, R. Oechslin, and P. Wellig, "Numerical and experimental radar cross section analysis of the quadrocopter DJI Phantom 2," in *2015 IEEE Radar Conference*, Oct. 2015, pp. 463–468.

M. D. Shear and M. S. Schmidt, "White House Drone Crash Described as a U.S. Workers Drunken Lark," *The New York Times*, Jan. 2015. [Online]. Available: https://www.nytimes.com/2015/01/28/us/white-house-drone.html

J. E. Stailey and K. D. Hondl, "Multifunction Phased Array Radar for Aircraft and Weather Surveillance," *Proceedings of the IEEE*, vol. 104, no. 3, pp. 649–659, Mar. 2016.

B. Torvik, K. E. Olsen, and H. Griffiths, "Classification of Birds and UAVs Based on Radar Polarimetry," *IEEE Geoscience and Remote Sensing Letters*, vol. 13, no. 9, pp. 1305–1309, Sep. 2016.

S. Werth, "Evaluating features for broad species based classification of bird observations using dual-polarized doppler weather radar," *Masters Theses*, Jan. 2016. [Online]. Available: https://scholarworks.umass.edu/masters_theses_2/381